SPECIAL TOPIC — International Conference on Nanoscience & Technology, China 2013

Nonlinear dynamic characteristics and optimal control of a giant magnetostrictive film-shaped memory alloy composite plate subjected to in-plane stochastic excitation*

Zhu Zhi-Wen(竺致文)[a)b)], Zhang Qing-Xin(张庆昕)[a)], and Xu Jia(许 佳)[a)b)†]

[a)] *Department of Mechanics, Tianjin University, Tianjin* 300072, *China*
[b)] *Tianjin Key Laboratory of Nonlinear Dynamics and Chaos Control, Tianjin* 300072, *China*

(Received 4 September 2013; revised manuscript received 5 January 2014; published online 10 June 2014)

The nonlinear dynamic characteristics and optimal control of a giant magnetostrictive film (GMF)-shaped memory alloy (SMA) composite plate subjected to in-plane stochastic excitation are studied. GMF is prepared based on an SMA plate, and combined into a GMF–SMA composite plate. The Van der Pol item is improved to explain the hysteretic phenomena of GMF and SMA, and the nonlinear dynamics model of a GMF–SMA composite cantilever plate subjected to in-plane stochastic excitation is developed. The stochastic stability of the system is analyzed, and the steady-state probability density function of the dynamic response of the system is obtained. The condition of stochastic Hopf bifurcation is discussed, the reliability function of the system is provided, and then the probability density of the first-passage time is given. Finally, the stochastic optimal control strategy is proposed by the stochastic dynamic programming method. Numerical simulation shows that the stability of the trivial solution varies with bifurcation parameters, and stochastic Hopf bifurcation appears in the process; the system's reliability is improved through stochastic optimal control, and the first-passage time is delayed. A GMF–SMA composite plate combines the advantages of GMF and SMA, and can reduce vibration through passive control and active control effectively. The results are helpful for the engineering applications of GMF–SMA composite plates.

Keywords: giant magnetostrictive film, shape memory alloy, composite cantilever plate, stochastic Hopf bifurcation, optimal control

PACS: 82.40.Bj, 47.20.Ky, 05.10.Gg, 05.45.–a **DOI:** 10.1088/1674-1056/23/8/088201

1. Introduction

Shape memory alloy (SMA) is a kind of smart material. It has been widely used in the engineering field. SMA has many special properties, such as shape memory, large damping, and super-elasticity. However, its application is hampered by its long response time. For improving the response, giant magnetostrictive film (GMF) is combined with SMA into a GMF–SMA composite material. GMF has many special properties, such as giant strain, rapid response, and excellent control precision, which can be used to control structure vibration effectively. A GMF–SMA composite plate combines the advantages of GMF and SMA, as well as reduces the vibrations in both passive control and active control effectively.

Numerous researchers have studied SMA plates and GMFs. Balapgol *et al*. studied the natural frequencies of a multilayer SMA laminated composite cantilever plate.[1] Roland *et al*. proposed a new multilayered nanostructured composite material produced by assembling SMA-treated thin plates.[2] Daghia *et al*. analyzed the active shape change of an SMA hybrid composite plate.[3] Ibuki *et al*. designed a kind of plate-type actuator using SMA wire for assistant artificial heart muscle.[4] In GMF field, Jia *et al*. developed a nonlinear magnetomechanical coupling model of GMF in low magnetic field.[5] Yang *et al*. proposed a kind of dynamic model of a magnetic system constructed with GMF using an element-free Galerkin method.[6] Masuda *et al*. created a highly responsive composite mover device constructed with positive and negative GMFs.[7] Tiercelin *et al*. used GMF to achieve the nonlinear actuation of cantilevers, and studied the response of the system in sub-harmonic excitation.[8] Although various achievements have been reported, the theoretical results of GMF–SMA composite plate are not adequate.

This paper aims to offer a kind of analysis method to solve the nonlinear dynamical characteristics and optimal control of a GMF–SMA composite cantilever plate subjected to in-plane stochastic excitation. The Van der Pol item is improved to explain the hysteretic loops of SMA and GMF. The nonlinear dynamic model of a GMF–SMA composite cantilever plate subjected to in-plane stochastic excitation is developed, and the stochastic bifurcation characteristics of the system are an-

*Project supported by the National Natural Science Foundation of China (Grant Nos. 11272229 and 11302144), the Ph. D. Programs Foundation of the Ministry of Education of China (Grant No. 20120032120006), and the Tianjin Research Program of Application Foundation and Advanced Technology, China (Grant No. 13JCYBJC17900).

†Corresponding author. E-mail: xujiatju@163.com

© 2014 Chinese Physical Society and IOP Publishing Ltd

alyzed. Finally, the stochastic optimal control strategy is proposed to improve the system's reliability.

2. Hysteretic nonlinear model of a GMF–SMA composite plate subjected to in-plane stochastic excitation

The structure of a GMF–SMA composite cantilever plate is shown in Fig. 1. The structure can be simplified into a single SMA plate since the thickness of SMA is 150 μm and that of GMF is only 10 nm–100 nm. The strain–stress curves of SMA are shown in Fig. 2.

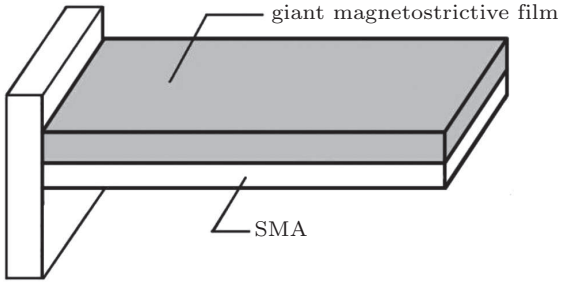


Fig. 1. Structure of a GMF–SMA composite cantilever plate.

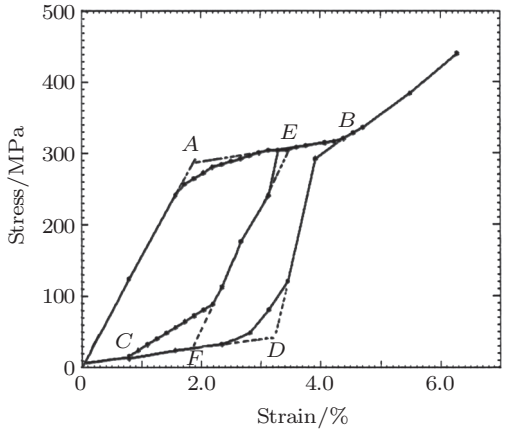


Fig. 2. Strain–stress curves of SMA.

Most of the SMA models are founded on thermodynamics theory and micromechanics theory, in which the percentage content of martensite is taken to be a main variable of the stress–strain equation. As a result, those SMA models are mostly shown to be equations with subsection functions or double integral functions, which are hard to analyze in theory.[9–11] Usually, research results can only be obtained by numerical or experimental methods. In this study, an improved Van der Pol hysteretic model is introduced to describe the hysteretic nonlinear characteristics of the strain–stress curves of SMA as follows:

$$\sigma = f_1(\varepsilon) + f_2(\varepsilon) = a_1\varepsilon - a_2\varepsilon^2 + a_3\varepsilon^3 + (a_4\varepsilon - a_5\varepsilon^2)\dot{\varepsilon}, \quad (1)$$

where σ is the stress, ε is the strain, a_i $(i = 1 \sim 5)$ are the coefficients, $f_1(\varepsilon) = a_1\varepsilon - a_2\varepsilon^2 + a_3\varepsilon^3$ is the skeleton curve of the hysteretic loop, $f_2(\varepsilon) = (a_4\varepsilon - a_5\varepsilon^2)\dot{\varepsilon}$ is the Van der Pol item, which describes the difference between the skeleton curve and the hysteretic loop.

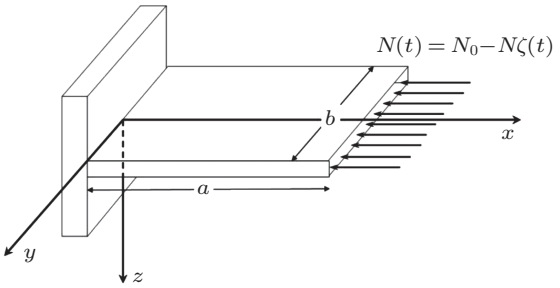


Fig. 3. Mechanical model of the GMF–SMA composite cantilever plate.

The mechanical model of the GMF–SMA composite cantilever plate subjected to in-plane stochastic excitation is shown in Fig. 3, where $p(t)$ is the in-plane excitation, $p(t) = p_0 + p'\xi(t)$, p_0 is the initial excitation, p' is the coefficient, $\xi(t)$ is the standard Gauss white noise whose mean is zero and intensity is two-dimensional (2D). Thus, the dynamical equation of a GMF–SMA cantilever plate subjected to in-plane stochastic excitation is as follows:

$$D\nabla^4 w + \rho h\frac{\partial^2 w}{\partial t^2} + \bar{\mu}\frac{\partial w}{\partial t} = \frac{\partial^2\phi}{\partial y^2}\frac{\partial^2 w}{\partial x^2} - 2\frac{\partial^2\phi}{\partial x\partial y}\frac{\partial^2 w}{\partial x\partial y} + \frac{\partial^2\phi}{\partial x^2}\frac{\partial^2 w}{\partial y^2} + p(t), \quad (2)$$

where D is the bending rigidity, $D = Eh^3/12(1-\nu^2)$, E is the Young's modulus, $E = \mathrm{d}\sigma/\mathrm{d}\varepsilon \approx a_1$,$h$ is the plate thickness, ν is the Possion ratio, $w = w(x,y,t)$ is the vibration mode of the GMF–SMA composite cantilever plate,

$$\nabla^4 = \frac{\partial^4}{\partial x^4} + 2\frac{\partial^4}{\partial x^2\partial y^2} + \frac{\partial^4}{\partial y^4},$$

ρ is the plate density, $\bar{\mu}$ is the damping coefficient, ϕ is the stress function and can be defined as follows:

$$\nabla^4\phi = Eh\left[\left(\frac{\partial^2 w}{\partial x\partial y}\right)^2 - \frac{\partial^2 w}{\partial x^2}\frac{\partial^2 w}{\partial y^2}\right]. \quad (3)$$

The boundary conditions of the SMA cantilever plate can be written as follows:

$$\begin{aligned}
&x = 0 : w = v = u = \phi_y = \phi_x = 0,\\
&x = \bar{a} : N_{xx} = N_{xy} = M_{xx} = M_{xy} - \bar{c}_1 P_{xy} = \bar{Q}_x = 0,\\
&y = 0 : N_{xy} = M_{yy} = M_{xy} - \bar{c}_1 P_{xy} = \bar{Q}_y = 0,\\
&y = \bar{b} : N_{xy} = M_{yy} = M_{xy} - \bar{c}_1 P_{xy} = \bar{Q}_y = 0,\\
&\int_{-h/2}^{h/2} N_{yy}\big|_{y=0,\bar{b}}\,\mathrm{d}z = \pm\int_{-h/2}^{h/2}(F_0 + F_1\cos\Omega_1 t)\,\mathrm{d}z,
\end{aligned}$$

where

$$\bar{Q}_x = Q_x + \frac{\partial M_{xy}}{\partial y} - \bar{c}_2 R_x + \bar{c}_1\left(\frac{\partial P_{xx}}{\partial x} + \frac{\partial P_{xy}}{\partial y}\right),$$

$$\bar{Q}_y = Q_y + \frac{\partial M_{xy}}{\partial x} - \bar{c}_2 R_y + \bar{c}_1 \left(\frac{\partial P_{yy}}{\partial y} + \frac{\partial P_{xy}}{\partial x} \right).$$

Thus, the vibration mode $w(x,y,t)$ can be assumed to be

$$w_0 = u_1 X_1(x) Y_1(y) + u_2 X_2(x) Y_1(y), \tag{4}$$

where

$$\begin{aligned}
&X_i(x) = \sin\lambda_i x - \sinh\lambda_i x + \bar{\alpha}_i(\cosh\lambda_i x - \cos\lambda_i x),\\
&Y_i(x) = \sin\mu_i y - \sinh\mu_i y + \bar{\beta}_i(\cosh\mu_i y + \cos\mu_i y),\\
&\cos\lambda_i\bar{a}\cosh\lambda_i\bar{a} + 1 = 0, \quad \cos\mu_i\bar{b}\cosh\mu_i\bar{b} + 1 = 0,\\
&\bar{\alpha}_i = \frac{\sinh\lambda_i\bar{a} + \sin\lambda_i\bar{a}}{\cosh\lambda_i\bar{a} + \cos\lambda_i\bar{a}}, \quad \bar{\beta}_i = \frac{\sinh\mu_i\bar{b} - \sin\mu_i\bar{b}}{\cosh\mu_i\bar{b} - \cos\mu_i\bar{b}}.
\end{aligned}$$

The differential equation of the vibration amplitude can be solved by Galerkin's method as follows:

$$\begin{cases}
\ddot{u}_1 + \mu\dot{u}_1 + k_1 u_1 - \alpha_1 u_1^2 + \gamma u_1 u_2^2 + \alpha_2 u_1^3\\
\quad + (\alpha_3 u_1 - \alpha_4 u_1^2)\dot{u}_1 = f_1 u_1 \varsigma(t),\\
\ddot{u}_2 + \mu\dot{u}_2 + k_2 u_2 - \beta_1 u_2^2 + \gamma u_1^2 u_2 + \beta_2 u_2^3\\
\quad + (\beta_3 u_2 - \beta_4 u_2^2)\dot{u}_2 = f_2 u_2 \varsigma(t),
\end{cases} \tag{5}$$

where

$$\begin{aligned}
&mu = \frac{\bar{\mu}}{\rho h}, \quad k_1 = \frac{D\pi^2(1/L^2 + 9/b^2)^2 - \pi^2/b^2 p_0}{\rho h},\\
&k_2 = \frac{D\pi^2(9/L^2 + 1/b^2)^2 - 9\pi^2/b^2 p_0}{\rho h},\\
&\alpha_1 = \frac{a_2\pi^4}{4\rho h L b}\left(\frac{27L}{b^3} + \frac{b}{L^3}\right),\\
&\beta_1 = \frac{a_2\pi^4}{4\rho h L b}\left(\frac{L}{b^3} + \frac{27b}{L^3}\right), \quad f_1 = \frac{\pi^2 p'}{\rho h b^2}, \quad f_2 = \frac{9\pi^2 p'}{\rho h b^2},\\
&\gamma = \frac{E\pi^4}{16\rho h L^2 b^2}\left[\frac{272}{(L^2+b^2)^2} + \frac{625}{(4L^2+b^2)^2} + \frac{625}{(L^2+4b^2)}\right],\\
&\alpha_2 = \frac{a_3\pi^4}{16\rho h L b}\left(\frac{81L}{b^5} + \frac{b}{L^5}\right), \quad \beta_2 = \frac{a_3\pi^4}{16\rho h L b}\left(\frac{L}{b^5} + \frac{81b}{L^5}\right),\\
&\alpha_3 = \frac{a_4\pi^2}{4\rho h L b}\left(\frac{27L}{b^2} + \frac{b}{L^2}\right), \quad \beta_3 = \frac{a_4\pi^2}{4\rho h L b}\left(\frac{L}{b^2} + \frac{27b}{L^2}\right),\\
&\alpha_4 = \frac{a_5\pi^4}{16\rho h L b}\left(\frac{81L}{b^3} + \frac{b}{L^3}\right), \quad \beta_4 = \frac{a_5\pi^4}{16\rho h L b}\left(\frac{L}{b^3} + \frac{81b}{L^3}\right).
\end{aligned}$$

3. Stochastic stability of the system

If we let $u_i = q_i$ and $\dot{u}_i = p_i$, then we can rewrite Eq. (5) as follows:

$$\begin{cases}
\dot{q}_1 = p_1,\\
\dot{p}_1 = -k_1 q_1 + \alpha_1 q_1^2 - \gamma q_1 q_2^2 - \alpha_2 q_1^3\\
\quad - (\mu + \alpha_3 q_1 - \alpha_4 q_1^2) p_1 + f_1 q_1 \varsigma(t),\\
\dot{q}_2 = p_2,\\
\dot{p}_2 = -k_2 q_2 + \beta_1 q_2^2 - \gamma q_1^2 q_2 - \beta_2 q_2^3\\
\quad - (\mu + \beta_3 q_2 - \beta_4 q_2^2) p_2 + f_2 q_2 \varsigma(t).
\end{cases} \tag{6}$$

The Hamiltonian function of Eq. (6) can be shown as follows:

$$\begin{aligned}
H = {} & \frac{1}{2}(p_1^2 + p_2^2) + \frac{1}{2}(k_1 q_1^2 + k_2 q_2^2)\\
& + \frac{1}{4}(\alpha_2 q_1^4 + \beta_2 q_2^4) + \frac{1}{2}\gamma q_1^2 q_2^2.
\end{aligned} \tag{7}$$

According to the quasi-nonintegrable Hamiltonian system theory, the Hamiltonian function $H(t)$ converges weakly in probability to a one-dimensional (1D) Ito diffusion process shown as follows:

$$\mathrm{d}H = m(H)\,\mathrm{d}t + \sigma(H)\,\mathrm{d}B(t), \tag{8}$$

where $B(t)$ is the standard Wiener process, $m(H)$ and $\sigma(H)$ are the drift and diffusion coefficients of the Ito stochastic process, which can be obtained through a stochastic averaging method:

$$\begin{aligned}
m(H) = {} & \frac{\Phi_1}{32\pi k_1 k_2} H - \frac{\Phi_2}{384\pi k_1^2 k_2^2} H^2 + \frac{1}{8}\left(\frac{5\mu k_2^3\alpha_2 + 5\mu k_1^3\beta_2}{768 k_1^3 k_2^3}\right.\\
& + \frac{5\pi k_2^2\alpha_1\alpha_4 + \pi k_1^2\beta_1\alpha_4 - k_1^2\gamma\beta_4}{512\pi k_1^3 k_2^2} - \frac{\gamma\alpha_4}{256 k_1^2 k_2}\\
& \left. + \frac{5\mu\alpha_2 k_2^3 + 5\mu\beta_2 k_1^3}{1536\pi k_1^3 k_2^3} + \frac{\alpha_1\beta_4 k_2^3}{1024\pi k_1^2 k_2^3}\right) H^3,
\end{aligned} \tag{9}$$

$$\sigma^2(H) = \frac{(k_2 f_1^2 + k_1 f_2^2) D H^2}{8 k_1 k_2}, \tag{10}$$

where

$$\begin{aligned}
\Phi_1 = {} & (-16\pi\mu - 6\mu + 1) k_1 k_2 + 2\pi D(k_2 f_1^2 + k_1 f_2^2),\\
\Phi_2 = {} & -80\pi k_1 k_2^2\alpha_4 - 40 k_1^2 k_2\beta_4 + 6\pi k_2^2\mu\alpha_1 - 4\pi k_1 k_2\mu\gamma\\
& + 3 k_2^2\mu\alpha_1 - 2 k_1 k_2\mu\gamma - 32\pi k_1 k_2 d\gamma f_1 f.
\end{aligned}$$

3.1. Local stability

Based on the quasi-nonintegrable Hamiltonian system theory, the largest Lyapunov exponent of a linearized system is defined as follows:

$$\lambda = \lim_{t\to\infty} \frac{1}{t} \ln \|Z(t, z_0)\|. \tag{11}$$

The linearized Ito differential equation can be shown after the system has been linearized in the trivial solution $H = 0$ as follows:

$$\mathrm{d}H = m'(0) H\,\mathrm{d}t + \sigma'(0) H\,\mathrm{d}B(t). \tag{12}$$

Then the associated largest Lyapunov exponent is

$$\lambda = \lim_{t\to\infty} \frac{1}{t} \ln H^{1/2} = \frac{-16\pi\mu - 6\mu + 1}{64\pi}. \tag{13}$$

The local stochastic stability of the system can be discussed as follows.

(i) The trivial solution $H = 0$ is locally asymptotically stable if and only if $\lambda < 0$, which means that $-16\pi\mu - 6\mu + 1 < 64\pi$;

(ii) The trivial solution $H = 0$ is locally asymptotically unstable if and only if $\lambda > 0$, which means that $-16\pi\mu - 6\mu + 1 > 64\pi$;

(iii) Bifurcation should appear near the trivial solution $H = 0$ if and only if $\lambda = 0$, which means that $-16\pi\mu - 6\mu + 1 = 64\pi$.

3.2. Global stability

The largest Lyapunov exponent can only estimate the local stability. In this paper, the boundary classification method is used to analyze the global stability of the trivial solution. In general, the boundaries of the diffusion process are singular, and the boundary classification is often determined by the diffusion exponent, drift exponent, and characteristic value.

When $H \to 0$,

$$m(H) \to O(H), \quad \sigma^2(H) \to O(H^2),$$

then

$$\alpha_l = 2, \quad \beta_l = 1, \quad c_l = \frac{k_1 k_2(-16\pi\mu - 6\mu + 1)}{2\pi d(k_2 f_1^2 + k_1 f_2^2)} + 1,$$

where α_l is the diffusion exponent, β_l is the drift exponent, c_l is the characteristic value, l is the left boundary.

Thus, the left boundary $H = 0$ belongs to the first kind of singular boundary. According to the classification for singular boundary, we obtain the following points.

i) The left boundary $H = 0$ is repulsively natural if $c_l > 1$;

ii) The left boundary $H = 0$ is strictly natural if $c_l = 1$;

iii) The left boundary $H = 0$ is attractively natural if $c_l < 1$.

Similarly, the right boundary $H = \infty$ belongs to the second kind of singular boundary, when $H \to \infty$,

$$m(H) \to O(H^3), \quad \sigma^2(H) \to O(H^2).$$

Then

$$\alpha_r = 2, \quad \beta_r = 3, \quad m(+\infty) > 0,$$

where r is the right boundary. Thus, the right boundary $H = \infty$ is an entrance boundary.

The necessary and sufficient conditions for globally asymptotic stability of the trivial solution require that the left boundary be attractively natural and the right boundary be an entrance boundary. Thus, the trivial solution $H = 0$ is globally asymptotically stable if and only if $c_l < 1$, which means that $-16\pi\mu - 6\mu + 1 < 64\pi$. The influence of the characteristic value on the stability is shown in Fig. 4.

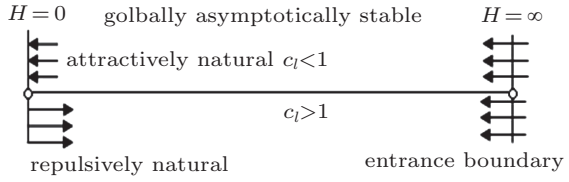


Fig. 4. Influence of the character value on stability.

4. Stochastic bifurcation and simulation

The averaged FPK equation of Eq. (8) is as follows:

$$\frac{\partial f}{\partial t} = -\frac{\partial}{\partial H}[m(H)f] + \frac{1}{2}\frac{\partial^2[\sigma^2(H)f]}{\partial H^2}, \tag{14}$$

where f is the probability density of the system response.

Thus,

$$\begin{aligned} f(H) &= \bar{A}\exp\left(-\int_0^H \left\{\left[\frac{\mathrm{d}\sigma^2}{\mathrm{d}t} - 2m(t)\right]/\sigma^2\right\}\mathrm{d}t\right) \\ &= \bar{A}H^{\eta}\exp[A_1 H + A_2 H^2], \end{aligned} \tag{15}$$

where $\bar{A}$ is a normalization constant,

$$\begin{aligned} \eta &= \frac{k_1 k_2(-16\pi\mu - 6\mu + 1)}{2\pi d(k_2 f_1^2 + k_1 f_2^2)} - 1, \\ A_1 &= \frac{\Phi_1}{24\pi k_1 k_2}(k_2 f_1^2 + k_1 f_2^2)D, \\ A_2 &= \frac{k_1 k_2}{(k_2 f_1^2 + k_1 f_2^2)D}\left(\frac{5\mu k_2^3\alpha_2 + 5\mu k_1^3\beta_2}{768 k_1^3 k_2^3}\right. \\ &\quad + \frac{5\pi k_2^2\alpha_1\alpha_4 + \pi k_1^2\beta_1\alpha_4 - k_1^2\gamma\beta_4}{512\pi k_1^3 k_2^2} - \frac{\gamma\alpha_4}{256 k_1^2 k_2} \\ &\quad \left. + \frac{5\mu\alpha_2 k_2^3 + 5\mu\beta_2 k_1^3}{1536\pi k_1^3 k_2^3} - \frac{\alpha_1\beta_4 k_2^3}{1024\pi k_1^2 k_2^3}\right). \end{aligned}$$

From Eq. (15), we find the following points.

(I) H^{η} decreases as H increases since $\eta < 0$;

(II) $\eta = 0$ when

$$-16\pi\mu - 6\mu + 1 = \frac{2\pi(k_2 f_1^2 + k_1 f_2^2)}{k_1 k_2},$$

then $H^{\eta} = 1$, and the stationary probability density of the system response $f(H)$ is determined by the item $\exp[A_1 H + A_2 H^2]$.

$$\frac{2\pi(k_2 f_1^2 + k_1 f_2^2)}{k_1 k_2} > 0$$

since $k_i > 0$. Thus,

$$-16\pi\mu - 6\mu + 1 = \frac{2\pi(k_2 f_1^2 + k_1 f_2^2)}{k_1 k_2}$$

means that μ, f_1, f_2 are all small enough. In this case especially, if $A_1 > 0$ and $A_2 < 0$, the stationary probability density will first increase, then decrease when H increases. It means that a limit loop will appear in the stationary probability density;

(III) For a linear damping system especially, the nonlinear damping coefficients A_1 and A_2 are both zero. It means that $f(H)$ is determined only by the item H^{η}, and will decrease when H increases. Thus, the origin (0, 0), which means the trivial solution $H = 0$, should have the highest probability density;

(IV) For a general system, $f(H)$ is determined by η, A_1, and A_2. When H is extremely small, the item H^{η} will be remarkable; when H increases, the item $\exp[A_1 H]$ will be remarkable; when H is large enough, the item $\exp[A_2 H^2]$ will

be remarkable. In this process, $f(H)$ first decreases, then increases, and finally decreases when H increases;

(V) Stochastic Hopf bifurcation appears when the bifurcation parameters η, A_1, and A_2 are varied.

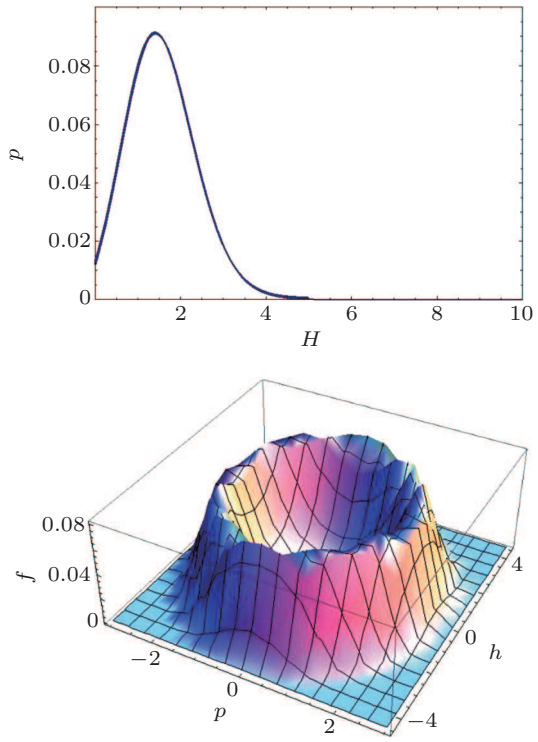


Fig. 5. (color online) Stationary probability density and joint probability density of the system when $\mu = 0$.

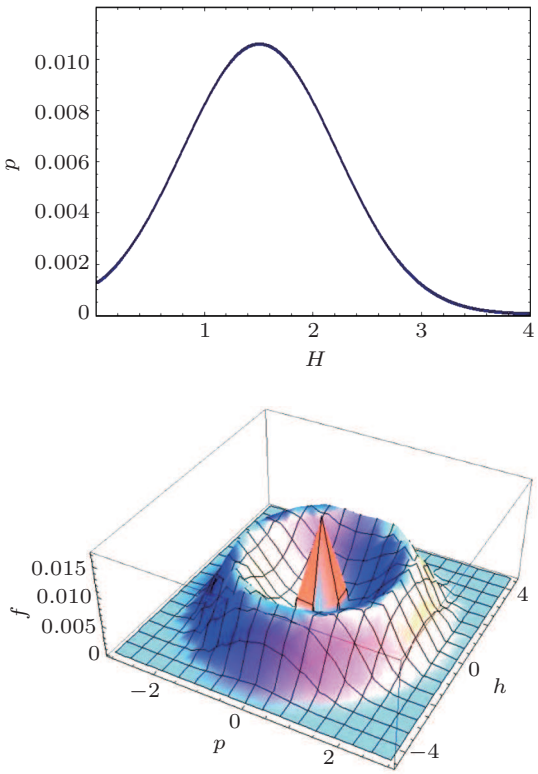


Fig. 6. (color online) Stationary probability density and joint probability density of the system when $\mu = 0.1$.

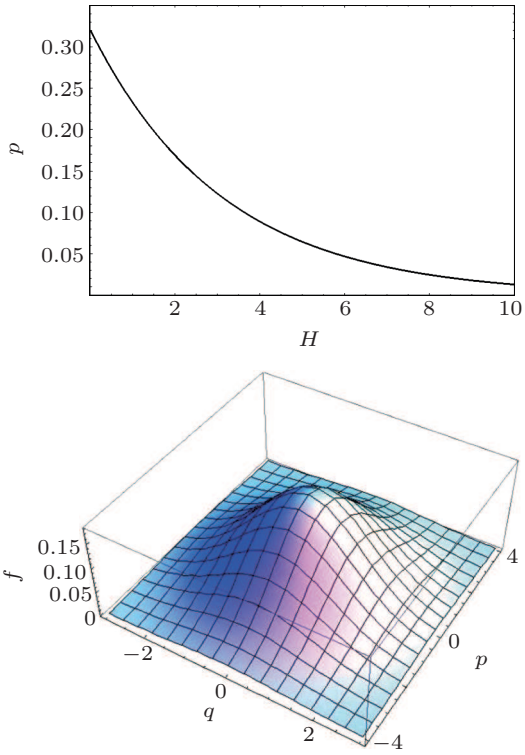


Fig. 7. (color online) Stationary probability density and joint probability density of the system when $\mu = 0.4$.

The results of the numerical simulation are shown in Figs. 5–7, where $\mu = 0.02$, $k_1 = 4$, $k_2 = 1$, $\gamma = 0.01$, $\alpha_1 = 0.5$, $\alpha_2 = 20$, $\alpha_3 = 1$, $\alpha_4 = 1$, $\beta_1 = 0.1$, $\beta_2 = 4$, $\beta_3 = 0.25$, $\beta_4 = 0.25$, $f_1 = 0.2$, and $f_2 = 1.8$.

From Figs. 5–7, we find the following results.

I) $p_i = 0$ and $q_i = 0$ when $H = 0$, so the trivial solution $H = 0$ corresponds to the origin (0, 0) in the probability density;

II) For a system with no damping, the set of those points of which the maximal probability density points form a loop, which is shown in Fig. 5; however, for a system with large damping, the origin point (0, 0) has the maximal probability density, which is shown in Fig. 7;

III) The steady-state probability density varies with parameter μ, and stochastic Hopf bifurcation appears in the process. The results of the simulation are in accordance with those of the theoretical analysis.

5. Stochastic optimal control of system reliability

From Section 4 it follows that the stochastic Hopf bifurcation appears when the bifurcation parameter μ varies. Stochastic Hopf bifurcation changes the system's motion, and reduces the system's reliability. In this section, the stochastic optimal control is introduced to improve the system's reliability.

The dynamic model of the controlled system can be shown as follows:

$$\begin{cases} \ddot{u}_1 + \mu\dot{u}_1 + k_1u_1 - \alpha_1u_1^2 + \gamma u_1u_2^2 + \alpha_2u_1^3 \\ \quad + (\alpha_3u_1 - \alpha_4u_1^2)\dot{u}_1 = f_1u_1\varsigma(\mathrm{t}) + F_1(t), \\ \ddot{u}_2 + \mu\dot{u}_2 + k_2u_2 - \beta_1u_2^2 + \gamma u_1^2u_2 + \beta_2u_2^3 \\ \quad + (\beta_3u_2 - \beta_4u_2^2)\dot{u}_2 = f_2u_2\varsigma(\mathrm{t}) + F_2(t), \end{cases} \tag{16}$$

where $F_1(t)$ and $F_2(t)$ are the active control forces. To a GMF–SMA composite cantilever plate, the active control force is supplied by a magnetic field.

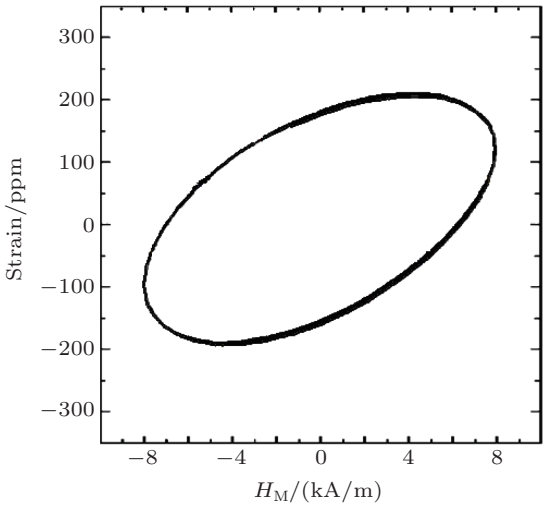


Fig. 8. Strain–MFI curves of GMF.

The strain-magnetic field intensity (MFI) curves of GMF are shown in Fig. 8. Like SMA, the strain–MFI curves of GMF can be expressed as follows:

$$H_{\mathrm{M}} = c_1\varepsilon - c_2\varepsilon^2 + c_3\varepsilon^3 + (c_4\varepsilon - c_5\varepsilon^2)\dot{\varepsilon}, \tag{17}$$

where c_i $(i = 1 \sim 5)$ are the coefficients.

According to the quasi-Hamiltonian theory, the 1D Ito diffusion process of Eq. (16) can be shown as follows:

$$\mathrm{d}H = \left[m(H) + \left\langle F(t)\frac{\partial H}{\partial p}\right\rangle\right]\mathrm{d}t + \sigma(H)\,\mathrm{d}B(t), \tag{18}$$

where

$$\left\langle F(t)\frac{\partial H}{\partial p}\right\rangle = \frac{1}{T(H)}\int_{\Gamma} F(t)\,\mathrm{d}q,$$

and

$$T(H) = \int_{\Gamma}\frac{1}{p}\,\mathrm{d}q, \quad \Gamma = \left\{q\middle|\,\frac{1}{2}kq^2 \le H\right\}.$$

The reliability function $R(H,t)$ of the system is determined in the dynamic programming principle shown as follows:

$$\begin{aligned}\frac{\partial R}{\partial t} = -\inf_{F}\Bigg\{&x^{\mathrm{T}}A^{\mathrm{T}}\frac{\partial R}{\partial x} + F^{\mathrm{T}}\bar{D}^{\mathrm{T}}\frac{\partial R}{\partial x} \\ &+ \frac{1}{2}(\sigma\sigma^{\mathrm{T}})_{ij}\frac{\partial^2 R}{\partial x_i\partial x_j} + x^{\mathrm{T}}Qx + F^{\mathrm{T}}RF\Bigg\}.\end{aligned} \tag{19}$$

Considering the average fist-passage time as the performance index:

$$J(F) = E[T(X,F)], \tag{20}$$

where T is the fist-passage time, and F^* is the optimal control when $J(F^*) = \inf_{F\in U} J(F)$.

The optimal control force F^* should make the reliability function maximal, so it can be determined as follows:

$$F^* = -\frac{1}{2}R^{-1}\bar{D}^{\mathrm{T}}\frac{\partial R}{\partial x}. \tag{21}$$

$\varepsilon = \sigma/E = F^*(t)/E\bar{A}$ can be obtained when the control force $F(t)$ is determined, where σ is the stress, E is the modulus of elasticity, $\bar{A}$ is the area of the cross section of GMF. Thus, the intensity of control magnetic field H_{M} can be given according to Eq. (17).

The probability density $p(H_0,t)$ of the first-passage time (FPT) of the controlled system is determined as follows:

$$p(H_0,T) = -\left.\frac{\partial R}{\partial t}\right|_{t=T}. \tag{22}$$

The results of the numerical simulation are shown in Figs. 9 and 10, where $H = 20$, $b = |\bar{D}|$=0/(1/3).

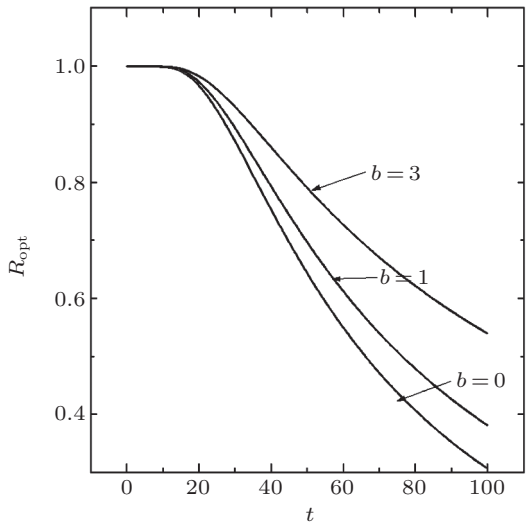


Fig. 9. Reliability of the system.

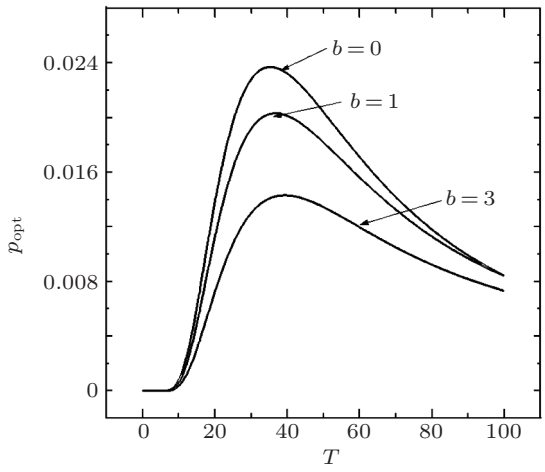


Fig. 10. Probability density of the first-passage time.

From Figs. 9 and 10, we find that

a) The reliability function $R(H,t)$ decreases as time increases;

b) The system's reliability is improved significantly as the control force increases, which indicates that the control strategy is effective;

c) The probability density of the first-passage time increases with time. The first-passage means that the system leaves the safe area, which causes the system to be unstable.

d) The first-passage time can be delayed through optimal control, which also means that the optimal control can enhance the system's reliability.

6. Conclusions

The nonlinear dynamic characteristics and optimal control of a giant magnetostrictive film (GMF)-shape memory alloy (SMA) composite cantilever plate subjected to in-plane stochastic excitation are studied. GMF is prepared based on an SMA plate, and combined into a GMF–SMA composite plate. The Van der Pol item is improved to explain the hysteretic phenomena of GMF and SMA, and the nonlinear dynamic model of a GMF–SMA composite cantilever plate subjected to in-plane stochastic excitation is developed. The stochastic stability of the system is analyzed, and the steady-state probability density function of the system's response is obtained. The condition of stochastic Hopf bifurcation is discussed, the reliability function of the system is solved, and then the probability density of the first-passage time is given. Finally, a stochastic optimal control strategy is proposed by a stochastic dynamic programming method. The results of the numerical simulation indicate that the stability of the trivial solution varies with bifurcation parameters, and stochastic Hopf bifurcation appears in the process; the system's reliability is improved through stochastic optimal control, and the first-passage time is delayed. A GMF–SMA composite plate combines the advantages of GMF and SMA, and can reduce the vibration through passive control and active control effectively. The results are helpful for the engineering applications of GMF–SMA composite plates.

References

[1] Balapgol B S, Bajoria K M and Kulkarni S A 2006 *Smart. Mater. Struct.* **15** 1021

[2] Roland T, Ya M and Retraint D 2004 *J. Mater. Sci. Technol.* **20** 55

[3] Daghia F, Inman D J and Ubertini F 2010 *Smart. Struct. Sys.* **6** 91

[4] Ibuki R, Maruyama S and Komiya A 2008 *J. Int. Mater. Sys. Struct.* **19** 359

[5] Jia Z Y, Liu W and Zhang Y S 2006 *Sensors and Actuators A* **128** 158

[6] Yang Q X, Chen H Y and Liu S Z 2006 *IEEE Trans. Magn.* **42** 939

[7] Masuda S, Matsumura Y and Nishi Y 2006 *Jpn. Inst. Metals* **70** 166

[8] Tiercelin N, Preobrazhensky V and Pernod P 2000 *J. Magn. Magn. Mater.* **210** 302

[9] Tanaka K 1986 *Res. Mech.* **18** 251

[10] Boyd J G and Lagoudas D C 1996 *In. J. Plast.* **12** 805

[11] Huang M and Brinson L C 1998 *J. Mech. Phys. Solids* **46** 1379